Nanotechnology **10** (1999) 273–277. Printed in the UK PII: S0957-4484(99)98802-5

Molecular dynamics simulations of the filling and decorating of carbon nanotubules

Zugang Mao, Ajay Garg and Susan B Sinnott†

Department of Chemical and Materials Engineering, The University of Kentucky, Lexington, KY 40506-0046, USA

E-mail: sinnott@engr.uky.edu

Received 29 October 1998

Abstract. Carbon nanotubes (CNTs) have been proposed as excellent materials for the construction of new, precisely tailored ultrafiltration membranes and as promising fibres for the construction of new, stronger composite materials. In this paper classical molecular dynamics simulations are used to investigate the potential use of CNTs in these applications. Functional groups have been covalently attached to the walls of CNTs to provide more extensive interactions between these new fibres and a polymer matrix. We examine the effects of these attachments on the mechanical properties of the tubules. The diffusive molecular flow of methane, ethane and ethylene through single tubules at room temperature are also studied. The simulations predict normal-mode molecular diffusion for methane. However, diffusion that is intermediate between normal-mode and single-file diffusion is predicted for ethane and ethylene. These diffusion results are found to be similar to results predicted for molecular diffusion in zeolites.

1. Introduction

Over the last few years the intense study of carbon nanotubules (CNTs) has highlighted their unique structural and electronic properties [1–4]. For example, CNTs can be single-walled (a single tubule) or multi-walled where 2–50 tubules are positioned concentrically within one another [1, 5]. The helical symmetry of the carbon atoms around the axis of the cylinder is indicated by two integers, (m, n), that represent the number of lattice vectors in the graphite plane used to make the tubule [6]. Numerous different chiral (m, n), 'zigzag' $(n, 0)$ and 'armchair' (n, n) helical configurations are possible. Calculations [7–12] and measurements [13, 14] have also determined that CNTs possess high Young's moduli, in the range of 1–5 TPa. Furthermore, because of their nanometre-scale size and hollow, cylindrical shape, CNTs have many potential applications [16] as molecular sieves, nano-test-tubes, and ultrafiltration membranes (membranes with pores on the order of 1–100 nm) [17]. Usually, such membranes are produced by only partially sintering a ceramic or by stretching a polymer [17]. In contrast, a CNT membrane, composed of tubules arranged in a bundle, would offer the advantages of fewer blocked pores and a narrower distribution of pore sizes than the usual techniques. It might function by physically excluding one molecular component from others in a mixture based on steric or size considerations or act as a selective adsorbent, preferentially adsorbing one component from a mixture on a thermodynamic basis. Finally, CNT bundles might act as agents of kinetic separation based on the differences in molecular diffusivities.

Because of their high stiffness in the direction of the tubule axis, nanotubules have also been proposed for use as fibres in the next generation of fibre-matrix composite materials [15]. Sometimes adhesion between the two phases of such composites is enhanced by chemically attaching polymer groups that act as 'tethers' to the fibres [18]. It is thought that these chemical attachments break at the fibre wall when the composite is deformed rapidly and disentangle from the surrounding matrix when the composite is deformed slowly. In either case, the attached group is crucial to the dissipation of energy that increases the overall resistance of the composite to failure. Recently, researchers at the University of Kentucky have worked to 'decorate' the walls of single-wall CNTs with dichlorocarbene [19, 20]. They are currently working to use standard methods to substitute polymer chains in place of the chlorine atoms. The first part of this paper summarizes the results of molecular dynamics simulations [21] to study the effect of covalent chemical functionalization on the stiffness of CNTs in the direction of the tubule axis.

The second part of this paper focuses on the 'filling' of CNTs with fluid molecules and their subsequent diffusion through the tubule. This is important as nanometre-scale fluids are expected to be fundamentally different from fluids in macroscopic porous systems. For example, bulk properties such as viscosity that are commonly used to characterize

† Webpage http://www.engr.uky.edu/CME/faculty/sinnott

fluids moving through a pipe are difficult to define or characterize at the nanometre scale. Consequently, several groups have used atomistic approaches to better understand the behaviour of molecules in nanometre-scale spaces. For example, Pederson and Broughton calculated the interaction energy between a HF molecule and a CNT with a diameter of about 8 Å using first principles density functional calculations [22]. This work showed that it was energetically favourable for the molecule to intercalate into the tubule walls. In addition, Tuzun *et al* have modelled the dynamic flow of helium and argon atoms through nanotubules to compare the results with the macroscopic analogues [23, 24].

However, diffusion in these nanometre-scale structures is expected to be most important for applications such as shape selective catalysis [25] and separations [26]. Nivarthi *et al* [27] and Gupta *et al* [28] have modelled the diffusion of methane and ethane, respectively, in $AlPO_4$-5. Their results showed that the mean-square displacement of methane was proportional to the square root of time, an indication of single-file diffusion. In contrast, the diffusion of ethane was intermediate between single-file and normal-mode (where the mean-square displacement is proportional to time) with the results depending strongly on molecular density. Finally, Sholl *et al* [29,30] have studied the concerted diffusion of molecular clusters in molecular sieves. They found that SF_6 and CCl_4 diffuse by concerted mechanisms involving all of the cluster molecules moving simultaneously. They also examined the diffusion of Ne, Ar, Kr, Xe, CH_4, $SnCl_4$, and $SnBr_4$ in $AlPO_4$-5 and predicted that as the atomic or molecular size increases, there is a transition from normal-mode diffusion to single-file diffusion. Similar phenomena are expected to occur in CNTs but there could be differences due to the shape of the nanometre-scale pore, including variations in the helical arrangement of the carbon atoms along the tubule axis, and the composition of the pore walls compared with $AlPO_4$-5.

2. Computational details

In both studies classical molecular dynamics simulations were used where Newton's equations of motion are integrated with a third-order Nordsieck predictor corrector [31]. Time steps of 0.15–0.25 fs were used in the simulations. The forces on the atoms were calculated using methods that vary with distance: short-range, chemical interactions were calculated using a reactive empirical bonding order hydrocarbon potential that realistically describes covalent bonding within both the molecules and CNTs. This method was originally developed by Brenner to study the chemical vapour deposition growth of diamond thin films [32]. It has also been successfully used to study reactions at surfaces [33, 34] and the structure and mechanical properties of CNTs [8, 12, 15, 21, 35, 36].

The long-range interactions were characterized with two different Lennard-Jones (LJ) potentials, one that was formulated for the study of liquid n-butane near its boiling point, termed LJ1 [37], and a LJ potential for generic hydrocarbon systems, referred to here as LJ2 [38]. The combined expression used to calculate the energy of the system in each case is thus

$$E_b = \sum_i \sum_{i<j} [V_r(r_{ij}) - B_{ij} V_a(r_{ij}) + V_{vdW}(r_{ij})] \quad (1)$$

where E_b is the binding energy, r_{ij} is the distance between atoms i and j, V_r is a pair-addictive term that consider the interatomic core–core repulsive interactions, and V_a is a pair-addictive term that models the attractive interactions due to the valence electrons. In addition, B_{ij} is a many-body empirical bond-order term that modulates valence electron densities and depends on atomic coordination and the bond angles. Finally, V_{vdw} is the contribution from the LJ potential and is only non-zero after the short-range REBO potential goes to zero.

The V_{vdw} is evaluated in two different ways. In the first approach, designated LJ1, it is evaluated as follows:

$$V_{vdW} = \begin{cases} 0.0 & r_{ij} \leqslant r_s \\ \{c_{3,k}(r_{ij} - r_k)^3 & \\ \quad +c_{2,k}(r_{ij} - r_k)^2 & \\ \quad +c_{1,k}(r_{ij} - r_k) + c_{0,k}\} & r_s \leqslant r_{ij} \leqslant r_m \\ \{4\varepsilon[(\sigma/r_{ij})^{12} - (\sigma/r_{ij})^6]\} & r_m \leqslant r_{ij} \leqslant r_b \end{cases} \quad (2)$$

where $c_{n,k}$ are cubic spline coefficients. The second implementation, designated LJ2, is determined as follows:

$$V_{vdW} = \begin{cases} 0.0 & r_{ij} \leqslant r'_s \\ \{c_{3,k}(r_{ij} - r_k)^3 & \\ \quad +c_{2,k}(r_{ij} - r_k)^2\} & r'_s \leqslant r_{ij} \leqslant r'_m \\ \{4\varepsilon[(\sigma/r_{ij})^{12} - (\sigma/r_{ij})^6]\} & r'_m \leqslant r_{ij} \leqslant r'_b. \end{cases} \quad (3)$$

The parameters for these two implementations appear in tables 1 and 2.

3. Results and discussion

3.1. The decoration of carbon nanotubules

To determine the effect of sp^3 'defect sites' caused by covalent functionalization of the tubule walls on CNT stiffness in the axial direction, simulations were performed [21] where functionalized and 'clean', unfunctionalized tubules were compressed. The functional groups were $H_2C{=}C$, selected to mimic the polymeric chains that will be attached to the tubules by University of Kentucky researchers. Tubules of different helical symmetries (armchair and zigzag) and various radii (0.339–1.665 nm) were studied. In the case of the armchair CNTs, 104 functional segments were attached to the tubule walls while 52 segments were attached to the zigzag tubule walls. This difference is necessary due to the changes in the helical symmetry in each case. About 3–5 unit cells at the ends of each tubule were held fixed while the next 12–15 unit cells had Langevin thermostats applied to them to maintain the temperature at 300 K. The atoms in the remaining 40–60 unit cells (including all the functional groups) had no constraints applied to them.

The tubules were compressed by moving the fixed atoms at one end of the tubule towards the other end in increments

Table 1. The parameters used for LJ1 from [37] in addition to standard cubic spline coefficients.

$\varepsilon_{cc} = 4.2038 \times 10^{-3}$ eV	$\varepsilon_{HH} = 5.8901 \times 10^{-3}$ eV	$\varepsilon_{CH} = \sqrt{(\varepsilon_{cc}\varepsilon_{HH})}$
$\sigma_{cc} = 0.337$ nm	$\sigma_{HH} = 0.291$ nm	$\sigma_{CH} = (\sigma_{cc} + \sigma_{HH})/2$
$r_{s,cc} = 0.228$ nm	$r_{s,HH} = 0.186$ nm	$r_{s,CH} = 0.220$ nm
$r_{m,cc} = 0.340$ nm	$r_{m,HH} = 0.300$ nm	$r_{m,CH} = 0.316$ nm
$r_{b,cc} = 1.00$ nm	$r_{b,HH} = 1.00$ nm	$r_{b,CH} = 1.00$ nm

Table 2. The parameters used for LJ2 from [38] in addition to standard cubic spline coefficients.

$\varepsilon_{cc} = 4.2038 \times 10^{-3}$ eV	$\varepsilon_{HH} = 5.8901 \times 10^{-3}$ eV	$\varepsilon_{CH} = \sqrt{(\varepsilon_{cc}\varepsilon_{HH})}$
$\sigma_{cc} = 0.337$ nm	$\sigma_{HH} = 0.291$ nm	$\sigma_{CH} = (\sigma_{cc} + \sigma_{HH})/2$
$r'_{s,cc} = 0.200$ nm	$r'_{s,HH} = 0.170$ nm	$r'_{s,CH} = 0.180$ nm
$r'_{m,cc} = 0.320$ nm	$r_{m,HH} = 0.276$ nm	$r'_{m,CH} = 0.298$ nm
$r'_{b,cc} = 1.00$ nm	$r'_{b,HH} = 1.00$ nm	$r'_{b,CH} = 1.00$ nm

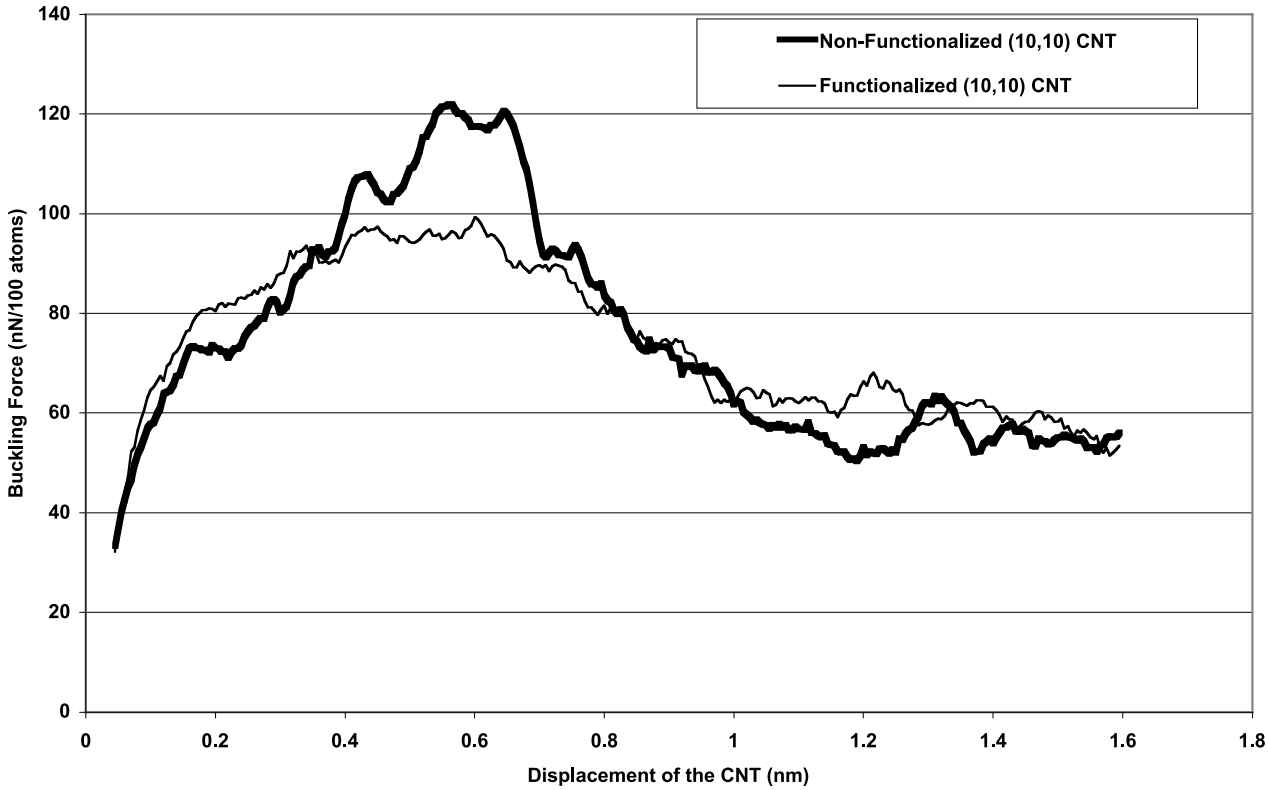

Figure 1. Force curve for the compression of functionalized and regular (10, 10) CNT.

of 0.005 nm and equilibrating the system for 400 steps. The forces on the atoms on one end of the tubule were summed to get the total force of compression during the 400 relaxation steps following each movement of the tubule end. However, only the average force from the last 100 steps was reported. These average forces included noise from thermal atomic vibrations, so additional averaging was performed to yield a smooth force versus displacement curve. Most of the simulations to study functionalization effects ran for about 80 ps.

As reported in other studies [8, 12, 35], these simulations predict the formation of buckles in the tubule to relieve the applied stress of compression. The oscillations of the force curve, shown in figure 1, reflect the formation of these buckles. Figure 1 shows the force curves obtained from the compression of both a functionalized and a clean (unfunctionalized) (10, 10) tubule. Comparing the two force curves we find that covalent functionalization of the tubule walls decreases the buckling force by 12.5%. In other words, the functionalized tubule is less stiff in the direction of the tubule axis than the clean tubule and so will deform more easily in a composite. When similar simulations were carried out on other armchair tubules ranging from a (5, 5) to a (25, 25), similar results were found [21]. In addition, studies on (10, 0) and (17, 0) tubules showed no dependence of the results on helical symmetry. Overall, functionalization decreases the stiffness of the tubule by an average value of about 15%.

3.2. The filling of carbon nanotubules

To model the diffusive flow of molecules through CNTs, 20–80 Å long tubules of various diameters were considered. The molecules were placed near the opening at one end (some

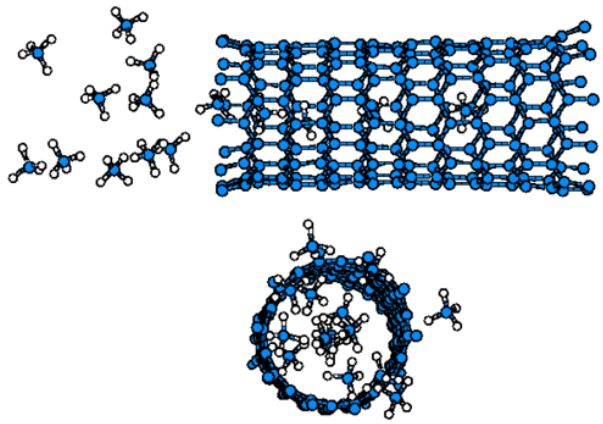

Figure 2. Snapshots from a molecular dynamics simulation of the diffusion of methane through a 20 Å long (10, 0) CNT.

slightly inside the tubule, some well outside the opening) and all of the atoms on the tubule walls had Langevin heat bath constraints applied to them. The system was then allowed to evolve in time with no additional constraints. These starting conditions correspond to an external molecular pressure gradient that has been shown experimentally to lead to diffusive flow. The average simulation ran for about 40 ps and the molecules were given no initial velocities aside from thermal values (their initial temperature was 300 K). Pore–pore correlation effects and changes in the initial temperature effects were not considered in this study.

First we considered the diffusive flow of a methane fluid with an initial density of 0.353 g cm^{-3} through a (10, 0) CNT with a diameter of 8.0 Å, shown in figure 2. Over time the molecules intercalated into the tubule and diffused down its length from the areas of high density to areas of low density. The average distance between the diffusing molecules was 5.2 Å using LJ1 and 4.1 Å using LJ2. The square of the average moving distance of methane was approximately proportional to time:

$$S^2 = 2At \tag{4}$$

where S is the average distance that the molecules move, A is the diffusion constant, and t is time. This corresponds to normal diffusion and the result is similar to the equation derived for molecular diffusion inside the molecular sieve $AlPO_4$-5 [39]. Using LJ2, the diffusive velocity of the molecules was significantly slower than using LJ1. The diffusion constant, A, in equation (4) was 3.8×10^{-4} cm^2 s^{-1} using LJ1 but only 8.5×10^{-3} cm^2 s^{-1} using LJ2. These values can be compared with the results of Keffer *et al* [39] who found a diffusion constant of 4.7×10^{-4} cm^2 s^{-1} for the diffusion of methane through $AlPO_4$-5. Thus the results using LJ2 show closer, but not perfect, agreement with these reported results. Possible reasons for the difference between our results and those of [39] are that the initial densities of methane in the two studies were slightly different and the diameters of the CNTs are slightly larger than in $AlPO_4$-5. The differences between the diffusion constants from LJ1 and LJ2 can be explained as follows. Because the molecules diffuse from areas of high density to areas of low density, the molecule–molecule interactions play an important role in diffusion although they are much smaller than the molecule–tubule interactions. The differences in long-range interactions between LJ1 and LJ2, as shown in tables 1 and 2, are largest in the distance region corresponding to molecule–molecule distances during diffusion. Thus, the methane molecules diffuse more quickly using LJ1 than LJ2. This also increases the average distance between the diffusing molecules leading to the difference in fluid density reported above.

Next we considered the diffusion of ethane molecules through the same (10, 0) tubules discussed above. The diffusion of ethane varied between single-file and normal-mode. Single-file diffusion is represented as follows:

$$S^2 = 2Bt^{1/2} \tag{5}$$

where B is the diffusion constant. When the diffusion data were fitted to equation (4) the diffusion constant was found to be 2.52×10^{-6} cm^2 s^{-1} using LJ1 and 2.55×10^{-5} cm^2 s^{-1} using LJ2. However, when fitted to equation (5), the calculated diffusion constant was found to be 8.85×10^{-10} cm^2 $s^{-0.5}$ using LJ1 and 1.58×10^{-10} cm^2 $s^{-0.5}$ using LJ2. In actual fact, neither equation provides a correct fit for the diffusion data for ethane, a finding that agrees with the results predicted for ethane diffusion through $AlPO_4$-5 in [39]. The findings for ethylene diffusion are similarly intermediate between single-file and normal-mode. The diffusion constants from fits to equation (4) are 3.35×10^{-5} cm^2 s^{-1} and 3.21×10^{-5} cm^2 s^{-1} using LJ1 and LJ2, respectively. The corresponding diffusion constants from fits to equation (5) are 9.50×10^{-10} cm^2 $s^{-0.5}$ and 1.93×10^{-10} cm^2 $s^{-0.5}$.

Finally, we considered the intercalation of molecules in tubules of smaller and larger diameters. When methane was allowed to diffuse through (5, 5) CNTs with diameters of 7.1 Å, the molecules could not pass each other because of the small tubule diameter. However, the diffusion behaviour was still unidirectional and easily fitted by equation (4) in agreement with the conclusions of Keffer *et al* [39]. When intercalation was studied in (16, 16) CNTs with diameters of 25 Å, there was no apparent motion of the molecules. Instead, they exhibited thermal vibrations and rotations during all of the 40 ps that this system was considered. This was due to the weak interactions between the fluid molecules and the atoms in the tubule walls in this case.

Thus, these results show that molecular interactions with the CNT walls can lead to molecular diffusion when the CNT diameters are small enough to result in strong interactions. As the tubule diameters increase, the molecule–tubule interactions weaken, resulting in no net motion on the timescales accessible through classical molecular dynamics simulations.

4. Conclusions

The effect of chemical covalent functionalization of the walls of CNTs was studied using classical molecular dynamics simulations. The results show that the introduction of sp^3-hybridized carbon defects due to chemical functionalization leads to degradation of the mechanical strength of single-walled CNTs by an average value of 15%. Helical symmetry

has little effect on the results of chemical functionalization. The diffusion of simple, multi-atomic fluids such as methane, ethane, and ethylene molecules through single, single-walled CNTs at room temperature was also investigated. Molecules inside the tubules tend to diffuse from areas of high density to areas of low density through interactions between the fluid molecules and the tubules. Methane exhibits normal diffusion regardless of the diameter of the tubule through which it is moving. However, the diffusion of ethane and ethylene is intermediate between single-file and normal mode for all the cases considered. Actual diffusion constants calculated depended heavily on the type of Lennard-Jones potential used to calculate the van der Waals interactions between the diffusing molecules and the tubule walls.

Acknowledgments

The authors gratefully acknowledge helpful discussions with Jie Han, Robert Haddon, Peter Eklund and Ernst Richter and financial support from the NASA-Ames Research Center (grant no NAG 201121).

References

[1] Iijima S 1991 *Nature* **354** 56
[2] Iijima S, Brabec C, Maiti A and Bernholc J 1996 *J. Chem. Phys.* **104** 2089
[3] Lambin Ph, Fonseca A, Vigneron J P, Nagy J B and Lucas A A 1995 *Chem. Phys. Lett.* **245** 85
[4] Mintmire J W and White C T 1996 *Synth. Met.* **77** 231
Mintmire J W, Dunlap B I and White C T 1992 *Phys. Rev. Lett.* **68** 631
[5] Ebbessen T W and Ajayan P M 1992 *Nature* **358** 220
Iijima S and Ichihashi T 1993 *Nature* **363** 603
Bethune D S, Kiang C H, de Vries M S, Gorman G, Savoy R, Vazques J and Beyers R 1993 *Nature* **363** 605
[6] Dresselhaus M S, Dresselhaus G and Eklund P C 1996 *Science of Fullerenes and Carbon Nanotubes* (San Diego, CA: Academic)
[7] Robertson D H, Brenner D W and Mintmire J W 1992 *Phys. Rev.* B **45** 12 592
[8] Yakobson B I, Brabec C J and Bernholc J 1996 *Phys. Rev. Lett.* **76** 2511
[9] Sinnott S B, White C T and Brenner D W 1995 *Science and Technology of Fullerene Materials (MRS Symp. Proc. 359)* ed P Bernier *et al* (Pittsburgh, PA: Materials Research Society) p 241
[10] Lu J P 1997 *Phys. Rev. Lett.* **79** 1297
[11] Wong E W, Sheehan P E and Lieber C M 1997 *Science* **277** 1971
[12] Cornwell C F and Wille L T 1997 *Solid State Commun.* **101** 555
[13] Ajayan P M, Stephan O, Colliex C and Trauth D 1994 *Science* **265** 1212
[14] Treacy M M J, Ebbesen T W and Gibson J M 1996 *Nature* **381** 678
[15] Sinnott S B, Shenderova O A, White C T and Brenner D W 1998 *Carbon* **36** 1
[16] Caruana C M 1997 *Chem. Eng. Prog.* **March** 17
[17] Cheryan M 1986 *Ultrafiltration Membranes* (Pennsylvania: Technomic Publishing Company) p 279
[18] Askeland D R 1994 *The Science and Engineering of Materials* 3rd edn (Boston, MA: PWS)
[19] Chen Y *et al* 1998 *J. Mater. Sci.* **13** 2423
[20] Chen J, Hamon M A, Hu H, Chen Y, Rao A M, Eklund E C and Haddon E C 1998 *Science* **282** 95
[21] Garg A, Han J and Sinnott S B 1998 *Chem. Phys. Lett.* **295** 273
[22] Pederson M R and Broughton J Q 1992 *Phys. Rev. Lett.* **69** 2689
[23] Tuzun R E, Noid D W, Sumpter B G and Merkle R C 1996 *Nanotechnology* **7** 241
[24] Tuzun R E, Noid D W, Sumpter B G and Merkle R C 1997 *Nanotechnology* **8** 112
[25] Carberry J J 1976 *Chemical and Catalytic Reaction Engineering* (New York: McGraw-Hill)
[26] de Vos R M and Verweij H 1998 *Science* **279** 1710
[27] Nivarthi S S, Mccormick A V and Davis H T 1994 *Chem. Phys. Lett.* **229** 297
[28] Gupta V, Nivarthi S S, Mccormick A V and Davis H T 1995 *Chem. Phys. Lett.* **247** 596
[29] Sholl D S and Fichthorn K A 1997 *Phys. Rev. Lett.* **79** 3569
[30] Sholl D S and Fichthorn K A 1997 *J. Chem. Phys.* **107** 4384
[31] Allen M P and Tildesley D J 1987 *Computer Simulation of Liquids* (New York: Oxford University Press)
[32] Brenner D W 1990 *Phys. Rev.* B **42** 9458
[33] Williams E R, Jones G C Jr, Fang L, Zare R N, Garrison B J and Brenner D W 1992 *J. Am. Chem. Soc.* **114** 3207
[34] Qi L and Sinnott S B 1998 *J. Vac. Sci. Technol.* A **16** 1293
[35] Garg A, Han J and Sinnott S B 1998 *Phys. Rev. Lett.* **81** 2260
[36] Robertson D H, Brenner D W and White C T 1992 *J. Phys. Chem.* **96** 6133
[37] Ryckaert J-P and Bellemans A 1975 *Chem. Phys. Lett.* **30** 123
[38] Moller M A, Tildsley D J, Kim K S and Quirke N 1991 *J. Chem. Phys.* **94** 8390
[39] Keffer D, McCormick A V and Davis H T 1996 *Mol. Phys.* **87** 367